

**SUPPLEMENTARY FILE**

**Band alignment and interfacial charge transfer in sol-gel derived anatase/rutile  
heterophase TiO<sub>2</sub>: Explaining the synergistic photocatalytic activity**

*Nimmy. A. V<sup>a</sup>, Anandakumar.V.M.<sup>bc</sup>, Biju. V<sup>a\*</sup>*

*<sup>a</sup>Department of Physics, University of Kerala, Kariavattom, Thiruvananthapuram, Kerala, 695581, India*

*<sup>b</sup>Department of Physics, Mahatma Gandhi College, Thiruvananthapuram, Kerala, 695004, India*

*<sup>c</sup>Department of Physics, VTMNSS Dhanuvachapuram, Thiruvananthapuram, Kerala, 695503, India*

*\*Author for correspondence: [bijunano@gmail.com](mailto:bijunano@gmail.com)*

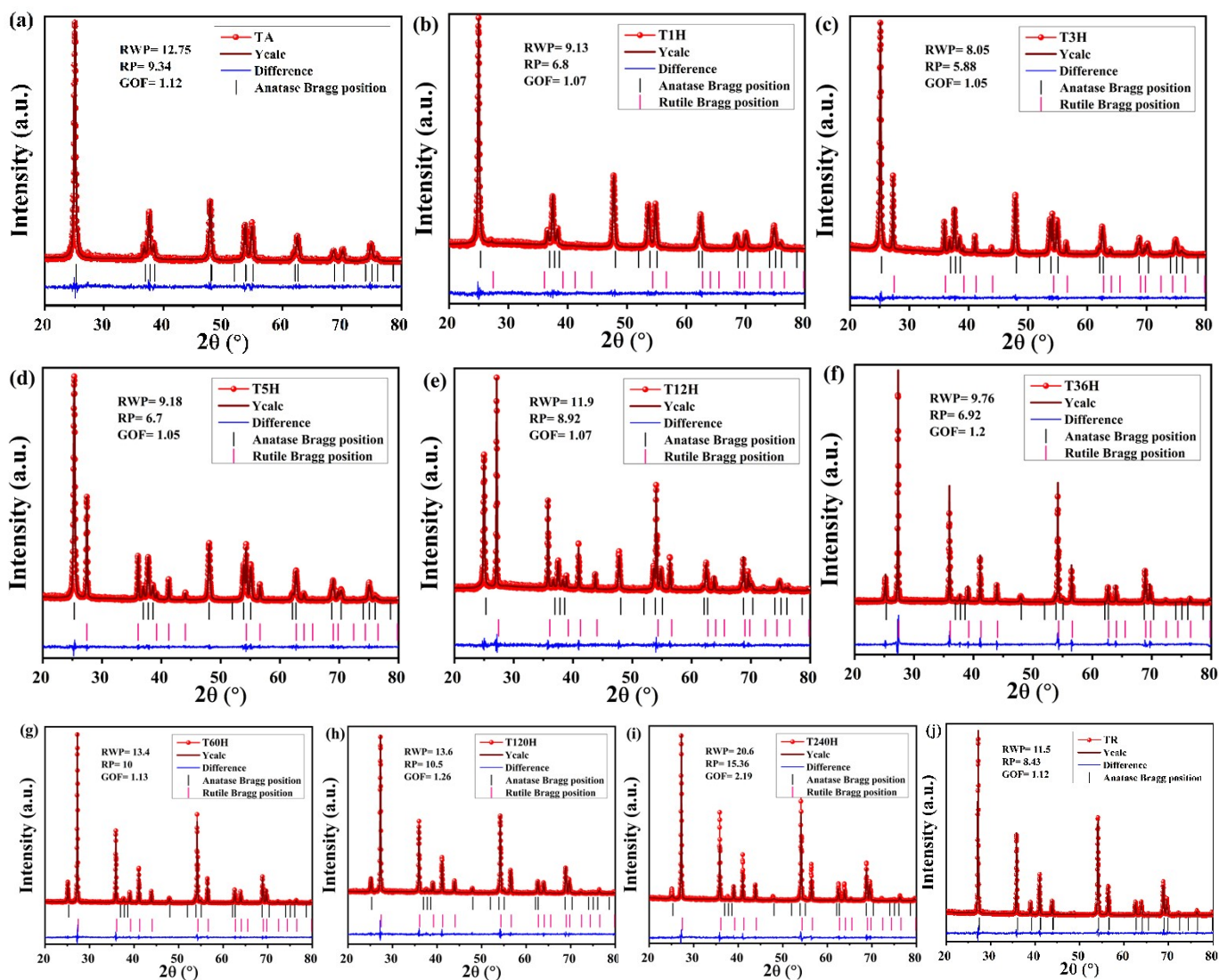


Fig. S1 Rietveld refinement patterns of the samples (a) TA, (b) T1H, (c) T3H, (d) T5H, (e) T12H, (f) T36H, (g) T60H, (h) T120H, (i) T240H and (j) TR

Table S1 Raman peak assignment table of the samples.

Assignments	Wavenumbers (cm <sup>-1</sup> ) of samples									
	TA	T1H	T3H	T5H	T12H	T36H	T60H	T120H	T240H	TR
E <sub>g</sub> (A)	141	141	141	141	141	141	-	-	-	-
B <sub>1g</sub> (R)	-	-	-	-	-	-	138	145	143	148
E <sub>g</sub> (A)	194	194	194	194	194	-	-	-	-	-
Multiphoton process (R)	-	-	-	-	-	234	227	233	234	240
B <sub>1g</sub> (A)	395	394	394	394	394	395	393	-	-	-
E <sub>g</sub> (R)	-	-	446	444	446	445	443	450	448	452
A <sub>1g</sub> /B <sub>1g</sub> (A)	514	513	513	513	515	513	513	518	-	-
A <sub>1g</sub> (R)	-	-	608	607	610	608	607	613	612	614
E <sub>g</sub> (A)	637	636	636	636	636	635	-	-	-	-
B <sub>2g</sub> (R)	-	-	-	-	-	827	827	834	838	834

(A) indicates for anatase and (R) for rutile

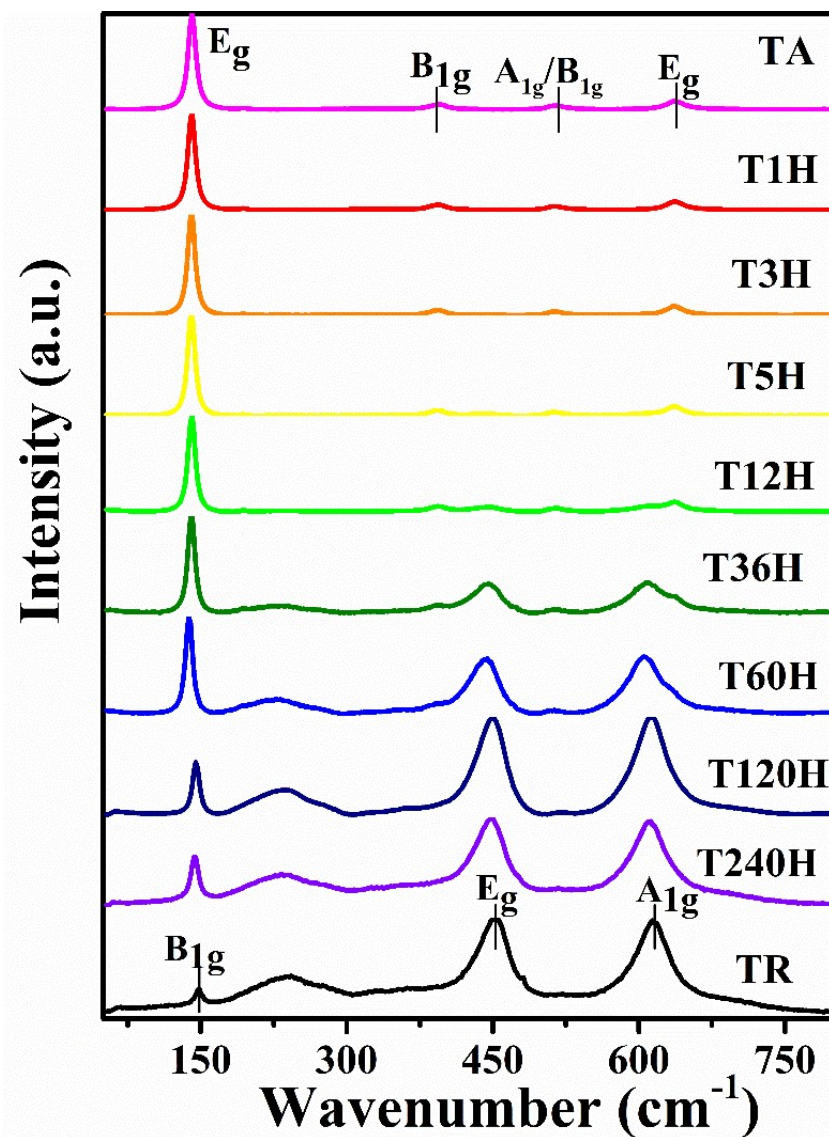


Fig. S2 Raman spectra of the TiO<sub>2</sub> samples

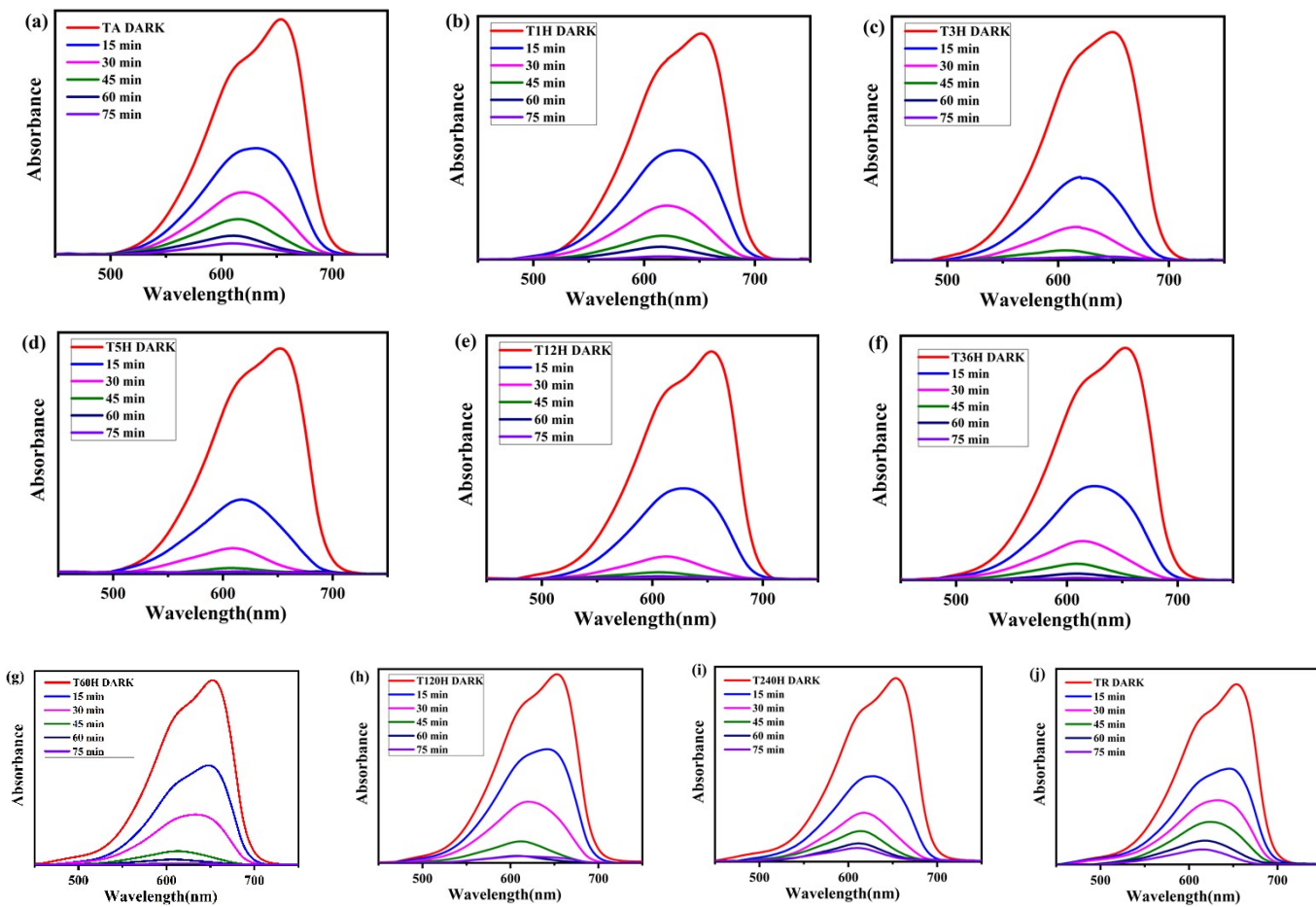


Fig. S3 Variation of absorbance of MB during solar photocatalytic degradation over time

Table S2 Photocatalytic performance of anatase/rutile TiO<sub>2</sub> in the previous reports.

Photocatalyst	Synthesis method	Organic pollutant	Photocatalytic parameters	D (%) / Rate constant	Reference
Anatase 0.03 g	Sol-gel technique	50 ml MB of 0.02 mM	Natural sunlight	84% after 75 minutes $2.24 \times 10^{-2} \text{ min}^{-1}$	1
A/R mixed phase (72% anatase) 0.03 g	Sol-gel technique	50 ml MB of 0.02 mM	Natural sunlight	99% after 75 minutes $6.25 \times 10^{-2} \text{ min}^{-1}$	1
Rutile 0.03 g	Sol-gel technique	50 ml MB of 0.02 mM	Natural sunlight	86% after 75 minutes $2.29 \times 10^{-2} \text{ min}^{-1}$	1
Anatase 0.03 g	Sol-gel technique	50 ml RhB of 0.02 mM	Natural sunlight	72% after 75 minutes $1.64 \times 10^{-2} \text{ min}^{-1}$	1
A/R mixed phase (72% anatase) 0.03 g	Sol-gel technique	50 ml RhB of 0.02 mM	Natural sunlight	77% after 75 minutes $2.05 \times 10^{-2} \text{ min}^{-1}$	1
Rutile 0.03 g	Sol-gel technique	50 ml RhB of 0.02 mM	Natural sunlight	31% after 75 minutes $0.49 \times 10^{-2} \text{ min}^{-1}$	1
Anatase 0.03 g	Sol-gel technique	50 ml phenol of 0.1 mM	Natural sunlight	60% after 75 minutes $1.39 \times 10^{-2} \text{ min}^{-1}$	1
A/R mixed phase (72% anatase) 0.03 g	Sol-gel technique	50 ml phenol of 0.1 mM	Natural sunlight	64% after 75 minutes $1.44 \times 10^{-2} \text{ min}^{-1}$	1
Rutile 0.03 g	Sol-gel technique	50 ml phenol of 0.1 mM	Natural sunlight	49% after 75 minutes $1.05 \times 10^{-2} \text{ min}^{-1}$	1
Anatase 0.5g/L	Peroxide gel route	100 ml MO of 0.01 mM	9 W UV lamp ~ 7 mW/cm <sup>2</sup>	60% after 180 minutes	2
A/R mixed phase (87.5% anatase) 0.5g/L	Peroxide gel route	100 ml MO of 0.01 mM	9 W UV lamp ~ 7 mW/cm <sup>2</sup>	73% after 180 minutes	2
A/R mixed phase (81.9% anatase) 0.5g/L	Peroxide gel route	100 ml MO of 0.01 mM	9 W UV lamp ~ 7 mW/cm <sup>2</sup>	55% after 180 minutes	2
A/R mixed phase (72.1% anatase) 0.5g/L	Peroxide gel route	100 ml MO of 0.01 mM	9 W UV lamp ~ 7 mW/cm <sup>2</sup>	8% after 180 minutes	2
A/R mixed phase (10.4% anatase)	Peroxide gel route	100 ml MO of 0.01 mM	9 W UV lamp ~ 7 mW/cm <sup>2</sup>	8% after 180 minutes	2

0.5g/L					
A/R mixed phase (87.5% anatase) 0.5g/L	Peroxide gel route	100 ml MO of 0.01 mM	150 W Xenon lamp 100 mW/cm <sup>2</sup>	90% after 60 minutes	2
A/R mixed phase (81.9% anatase) 0.5g/L	Peroxide gel route	100 ml MO of 0.01 mM	150 W Xenon lamp 100 mW/cm <sup>2</sup>	65% after 60 minutes	2
A/R mixed phase (72.1% anatase) 0.5g/L	Peroxide gel route	100 ml MO of 0.01 mM	150 W Xenon lamp 100 mW/cm <sup>2</sup>	45% after 60 minutes	2
A/R mixed phase (40% rutile) 0.4g/L	Solvent mixing and calcination of sol-gel derived anatase and rutile	75 ml MB 0.0064 μmol/L	15 W UV Lamp for 60 minutes	$2.3 \times 10^{-2} \text{ min}^{-1}$	3
A/R mixed phase (40% rutile) 1g/L BET surface area:218 m <sup>2</sup> /g	Hydrothermal	200 ml RhB 10 <sup>-6</sup> M	300 W UV Lamp	$1.1 \times 10^{-2} \text{ min}^{-1}$	4
A/R mixed phase (81% rutile) 1g/L BET surface area:49 m <sup>2</sup> /g	Hydrothermal	200 ml RhB 10 <sup>-6</sup> M	300 W UV Lamp	$1.7 \times 10^{-2} \text{ min}^{-1}$	4
A/R mixed phase (45% rutile) 1g/L BET surface area:233 m <sup>2</sup> /g	Spray drying of hydrothermally treated sol	200 ml RhB 10 <sup>-6</sup> M	300 W UV Lamp	$0.8 \times 10^{-2} \text{ min}^{-1}$	4
A/R mixed phase (74% rutile) 1g/L BET surface area:85 m <sup>2</sup> /g	Spray drying of hydrothermally treated sol	200 ml RhB 10 <sup>-6</sup> M	300 W UV Lamp	$2.3 \times 10^{-2} \text{ min}^{-1}$	4

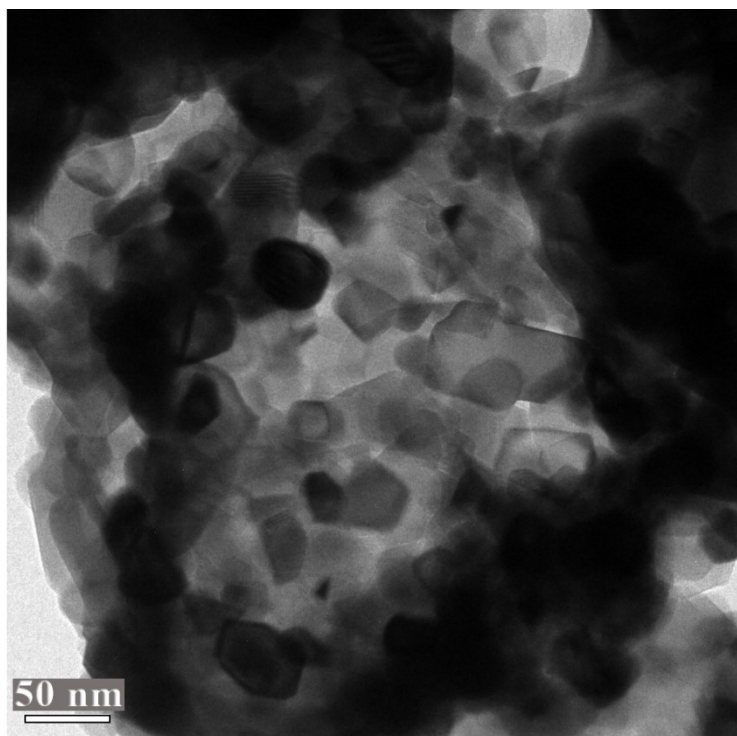


Fig. S4 HRTEM image of sample T12H

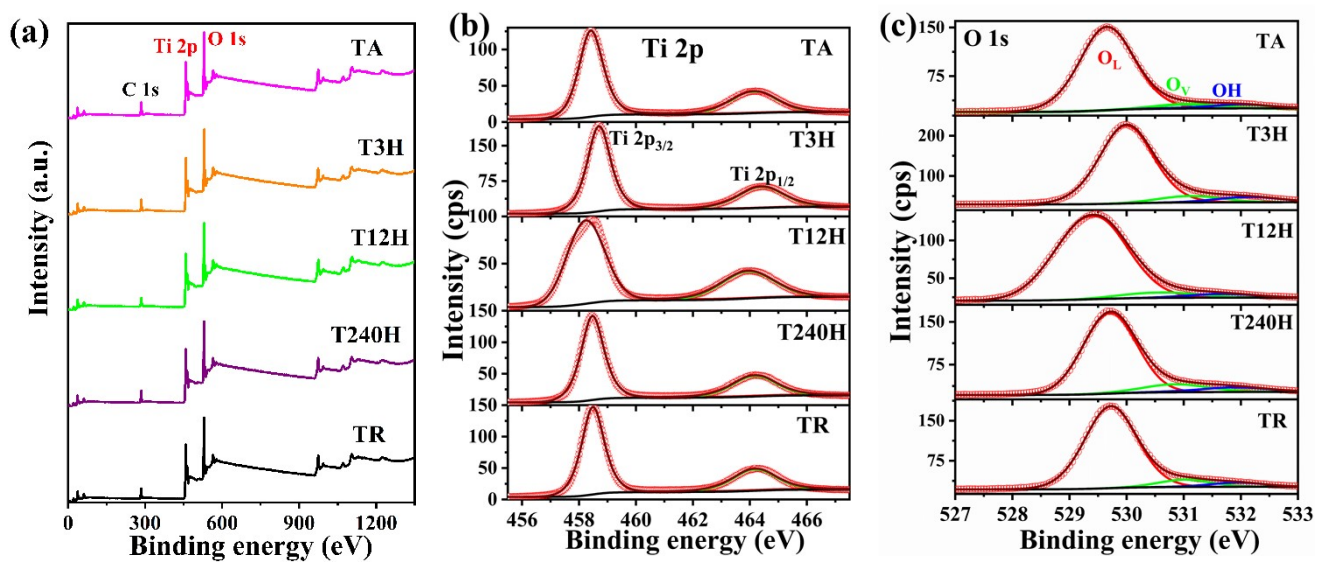


Fig. S5 (a) XPS survey spectrum (b) Ti 2p narrow scan and (c) O 1s narrow scan of TiO<sub>2</sub> samples TA, T3H, T12H, T240H and TR.



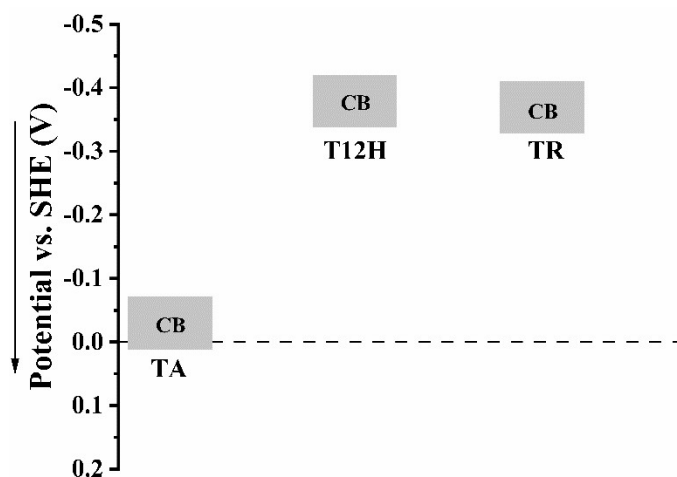


Fig. S6 Schematic diagram of band alignment potential of anatase (TA), rutile (TR) and anatase-rutile mixed sample (T12H) with respect to SHE.

### Measurement of Band offsets using XPS technique:

Kraut et al.<sup>5</sup>, developed a well-established method for determining the semiconductor interface potentials in a two-phase mixed sample with the help of XPS. We have adopted this method to determine the valence band offset at the interface of anatase and rutile phases by considering Ti 2p<sub>3/2</sub> core level energy as reference.<sup>5,6</sup> This method is based on the measurement of difference in binding energy of core level and valence band maximum.

The valence band offset ( $\Delta E_V$ ) values of anatase and rutile phases were calculated using the equation,

$$\Delta E_V = (E_{CL}^{anatase} - E_V^{anatase}) - (E_{CL}^{rutile} - E_V^{rutile}) - \Delta E_{CL} \quad (8)$$

Where,  $E_{CL}^{anatase}$  is the energy of a core level of the anatase

$E_V^{anatase}$  is the valence band maximum of the anatase

$E_{CL}^{rutile}$  is the energy of a core level of the rutile

$E_V^{rutile}$  is the valence band maximum of the rutile

$\Delta E_{CL} = E_{CL}^{anatase}(i) - E_{CL}^{rutile}(i)$ , core level energy difference of the anatase and rutile at the interface.<sup>5,6</sup>

Using this method, we tried to analyze the band alignment at the anatase/rutile interface of mixed phases T3H, T12H and T240H. For that purpose, the core level and VB XPS spectra of the pure phases, TA (anatase), TR (rutile) and three of the mixed phase samples with varying phase fraction were recorded using a Thermo scientific ESCALAB Xi<sup>+</sup> using Al K <sub>$\alpha$</sub>  X-ray (1486.6 eV). The instrumental set up mentioned in the experimental section in the manuscript.

From the VB XPS of the pristine phase samples (TA and TR),  $E_V^{anatase}$  and  $E_V^{rutile}$  were determined by extrapolating the lower band edge of VB XPS spectra to the baseline, as in Fig. 5(b). The obtained VB maximum value of  $E_V^{anatase} = 2.11$  eV and  $E_V^{rutile} = 2.25$  eV. The Ti 2p<sub>3/2</sub> core level energy of anatase (TA) and rutile (TR) phases are,  $E_{CL}^{anatase} = 458.41$  eV and  $E_{CL}^{rutile} = 458.48$  eV. Then,  $E_{CL}^{anatase} - E_V^{anatase}$  and  $E_{CL}^{rutile} - E_V^{rutile}$  values were estimated.

A notable peak broadening was found in the spectra of mixed phase samples (T3H, T12H and T240H). This broadening is due to the existence of anatase/rutile interfaces.<sup>6</sup> Hence, the Ti 2p<sub>3/2</sub> core level of mixed phase consisted of two components, corresponding to the Ti ions in the rutile and anatase crystal structures. So, this core level is deconvoluted into the corresponding pure phases, as shown in Fig. 5(a). The peaks were fitted with Voigt function profiles after subtracting the background with Smart function using the software Avantage, Thermo Fisher Scientific. This peak fitting was done by constraining the peak area ratio according to the estimated phase fraction while keeping least residual standard deviation (or residual error), which is the figure of merit used to evaluate the quality of fit. In a similar manner, we have deconvoluted the peaks in two different cases; with the rutile component at higher or lower binding energy region. For all the samples, this model gave a better fit

(least residual error) only when the rutile was at lower binding energy, as in Fig. 5(a). This method supported the findings on the study of Scanlon and coworkers.<sup>6</sup> The results of the curve fitting are included in Fig. 5(a). Then, difference in core level energies of the mixed phase at the interface,  $\Delta E_{CL} = E_{CL}^{anatase}(i) - E_{CL}^{rutile}(i)$ , was computed. The values of  $\Delta E_{CL}$  is tabulated in Table 3. Then, the valence band offset values were estimated using eqn (8). The estimated valence band offset between the anatase and rutile phases of T3H, T12H and T240H were 0.71, 0.83 and 0.50 eV respectively. It is clear that, VB of anatase lies at higher binding energy than that of rutile in the mixed samples. Using the optical bandgap values of these samples estimated from the UV-visible DRS analysis, we calculated the CB offset also. The obtained band alignment is shown in the Fig. 6. It is confirmed that, all these three samples show type II staggered band alignment with VB and CB of rutile lying above those of anatase as in Fig. 1. Hence the possible conduction electron transfer will be from the CB of rutile to anatase and the hole transfer from the VB of anatase to rutile.

## References:

- 1 A. V. Nimmy, A. Mahesh, V. M. Anandakumar and V. Biju, Revealing the role of defect-induced trap levels in sol-gel-derived TiO<sub>2</sub> samples and the synergistic effect of a mixed phase in photocatalytic degradation of organic pollutants, *J. Phys. Chem. Solids*, 2024, **185**, 111774.

- 2 B. Anitha and M. A. Khadar, Anatase-rutile phase transformation and photocatalysis in peroxide gel route prepared TiO<sub>2</sub> nanocrystals: Role of defect states, *Solid State Sci.*, 2020, **108**, 106392.
- 3 A. Zachariah, K. V. Baiju, S. Shukla, K. S. Deepa, J. James and K. G. K. Warner, Synergistic effect in photocatalysis as observed for mixed-phase nanocrystalline titania processed via sol-gel solvent mixing and calcination, *J. Phys. Chem. C*, 2008, **112**, 11345–11356.
- 4 S. Pal, A. M. Laera, A. Licciulli, M. Catalano and A. Taurino, Biphasic TiO<sub>2</sub> microspheres with enhanced photocatalytic activity, *Ind. Eng. Chem. Res.*, 2014, **53**, 7931–7938.
- 5 E. A. Kraut, R. W. Grant, J. R. Waldrop and S. P. Kowalczyk, Precise Determination of the Valence-Band Edge in X Ray Photoemission Spectra, *Phys. Rev. Lett.*, 1980, **44**, 1620.
- 6 D. O. Scanlon, C. W. Dunnill, J. Buckeridge, S. A. Shevlin, A. J. Logsdail, S. M. Woodley, C. R. A. Catlow, M. J. Powell, R. G. Palgrave, I. P. Parkin, G. W. Watson, T. W. Keal, P. Sherwood, A. Walsh and A. A. Sokol, Band alignment of rutile and anatase TiO<sub>2</sub>, *Nat. Mater.*, 2013, **12**, 798–801.